

Communication

Carbon Electrodes for K-Ion Batteries

Zelang Jian, Wei Luo, and Xiulei Ji

J. Am. Chem. Soc., **Just Accepted Manuscript** • DOI: 10.1021/jacs.5b06809 • Publication Date (Web): 02 Sep 2015

Downloaded from <http://pubs.acs.org> on September 3, 2015

Just Accepted

"Just Accepted" manuscripts have been peer-reviewed and accepted for publication. They are posted online prior to technical editing, formatting for publication and author proofing. The American Chemical Society provides "Just Accepted" as a free service to the research community to expedite the dissemination of scientific material as soon as possible after acceptance. "Just Accepted" manuscripts appear in full in PDF format accompanied by an HTML abstract. "Just Accepted" manuscripts have been fully peer reviewed, but should not be considered the official version of record. They are accessible to all readers and citable by the Digital Object Identifier (DOI®). "Just Accepted" is an optional service offered to authors. Therefore, the "Just Accepted" Web site may not include all articles that will be published in the journal. After a manuscript is technically edited and formatted, it will be removed from the "Just Accepted" Web site and published as an ASAP article. Note that technical editing may introduce minor changes to the manuscript text and/or graphics which could affect content, and all legal disclaimers and ethical guidelines that apply to the journal pertain. ACS cannot be held responsible for errors or consequences arising from the use of information contained in these "Just Accepted" manuscripts.



Carbon Electrodes for K-Ion Batteries

Zelang Jian, Wei Luo and Xiulei Ji*

Department of Chemistry, Oregon State University, Corvallis, Oregon, 97331-4003, United States

Supporting Information Placeholder

ABSTRACT: We, for the first time, report electrochemical potassium insertion in graphite in a non-aqueous electrolyte, which can exhibit a high reversible capacity of 273 mAh/g. *Ex situ* XRD studies confirm that KC_{36} , KC_{24} and KC_8 sequentially form upon potassiation while depotassiation recovers graphite through phase transformations in an opposite sequence. Graphite shows moderate rate capability and relatively fast capacity fading. In order to improve the performance of carbon KIB anodes, we synthesized a non-graphitic soft carbon that exhibits much superior cyclability and rate capability to graphite. This work may open up a new paradigm towards rechargeable K-ion batteries.

Demand for Li-ion batteries (LIBs) is rapidly increasing in powering electronic devices and vehicles.^{1,2} However, the scarcity and rising cost of lithium resources cause a concern on heavy reliance of LIBs.³ This is particularly true when considering stationary applications that are indispensable for deployment of renewable energy.² One of the basic requirements for stationary batteries is low cost upon scaling up, where the economies of scale should be applicable. This calls for alternative energy storage devices that are based on Earth-abundant elements.^{4,5} Along this line, recently, Na-ion batteries (NIBs) receive renewed attention because sodium occupy 2.3 wt.% in contrast to 0.0017 wt.% for lithium in Earth crust.⁶⁻⁹ Rapid progress has been made on the cathode side of NIBs, where layered metal oxides⁷⁻⁹ and polyanionic compounds¹⁰⁻¹² demonstrate encouraging capacity and cycling life. In fact, the hurdle of NIBs is on the anode side.¹³ In LIBs, graphite exhibits a reversible capacity of ~370 mAh/g by forming LiC_6 , the stage-one Li-graphite intercalation compound (GIC).^{14,15} Unfortunately, Na/graphite cells only deliver a maximum capacity of ~35 mAh/g by forming NaC_{64} unless solvent molecules are co-inserted or expanded graphite is used.¹⁶⁻¹⁸

Pure graphite's failure in NIBs may have discouraged progress in using graphite as an electrode in K-ion batteries (KIBs). Electrochemical potassium insertion into graphite was conducted in molten KF or KF/AlF_3 at above 700 °C.^{19,20} Wang *et al.* reported reversible electrochemical insertion of potassium into non-graphitic carbon nanofibers at room temperature.²¹ In fact, KC_8 , the stage-one K-GIC, as the first discovered alkali metal GIC, has been readily synthesized by potassium vapor transport or by soaking graphite in a non-

aqueous solution with potassium metal solvated.²²⁻²⁵ Surprisingly, it remains unknown whether K-GICs can be formed in an electrochemical K/graphite cell at room temperature. Like NIBs, the interests on KIBs originate from the abundance of potassium as it occupies 1.5 wt.% of Earth crust. Progress has been made on the cathode side of KIBs with Prussian blue and its analogues in both aqueous and non-aqueous electrolytes.^{26,27}

Here, we, for the first time, report electrochemical potassium storage properties of graphite. We selected a commercially available synthetic graphite (TIMCAL TIMREX SLP50), which exhibits a well-defined crystal structure as demonstrated in X-ray diffraction (XRD), transmission electron microscopy (TEM), and Raman Spectroscopy (Figure 1A and Figure S1). The K/graphite cells are assembled in an argon-filled glove box, with graphite as the working electrode, potassium metal (99.5%, Sigma-Aldrich) as the counter/reference electrode and 0.8 M KPF_6 (99.5%, Sigma-Aldrich) in 50:50 ethylene carbonate (EC, BASF) and diethyl carbonate (DEC, BASF).

We first attempt to probe the maximum capacity of graphite in KIBs at room temperature. We conducted galvanostatic potassiation/depotassiation (GPD) tests at C/40 (We define 1C for the current rate, at which the stoichiometry of KC_8 forms during one hour of potassiation of carbon electrodes.), where graphite exhibits surprisingly high capacities of 475 and 273 mAh/g in potassiation and depotassiation, respectively (Figure 1B). The depotassiation capacity is very close to the theoretical value of 279 mAh/g when KC_8 forms. The initial potassiation capacity is much larger than the theoretical capacity, which is responsible for the low initial Coulombic efficiency (CE) of 57.4%. Comparing potassiation potential profiles in the first two cycles show that the slope region from 1 to 0.4 V (all potentials are vs. K^+/K) only exists in the first cycle, which disappears in the second cycle. This is very similar to the first-cycle behavior of graphite anode in LIBs when solid electrolyte interphase (SEI) forms on graphite surface.^{28,29} The following less steep slope from 0.4 to 0.2 V in the first potassiation also contributes to the initial irreversible capacity as it is much diminished in the second cycle. On the other hand, the depotassiation potential profiles overlap very well in the first two cycles.

At C/40, the primary potassiation and depotassiation plateaus locate at 0.17 V and 0.27 V, respectively, thus resulting in a polarization of 0.1 V. To reveal the equilibrium

potential of potassium storage, we employed galvanostatic intermittent titration technique (GITT), where a constant current at $C/10$ is applied for 0.5 hr before cells rest at open circuit for 1 hr. As Figure 1C shows, the quasi-equilibrium potentials for both potassiation and depotassiation are close to 0.24 V, much higher than that of Li insertion in graphite, at ~ 0.1 V vs. Li^+/Li .¹⁵ The higher potassiation potential is practically critical as it relieves the risk of the dendrite formation on graphite surface. Besides the primary plateau, there exist other minor plateaus in GPD profiles, which are more evident in the dQ/dV profiles (We refer to the differential capacity as dQ/dV), i.e., O_2/R_2 and O_3/R_3 peaks (Figure 1D).

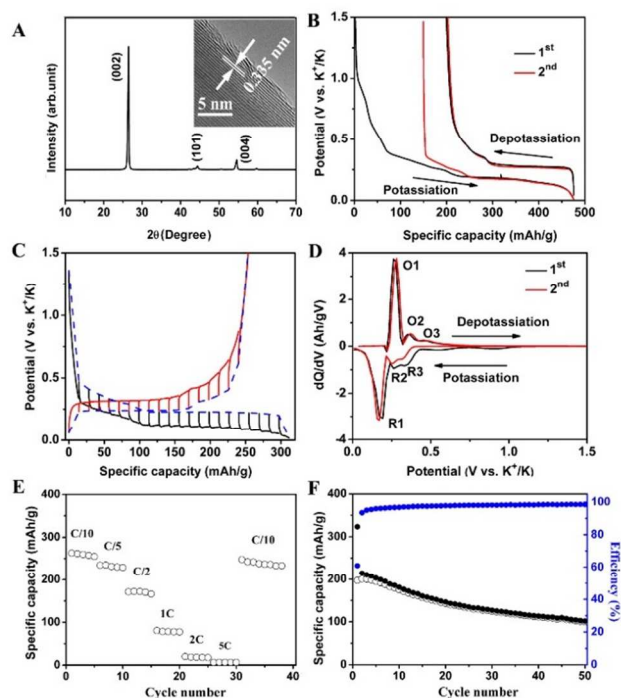


Figure 1. (A) XRD pattern of graphite. Inset: A TEM image of graphite. (B) GPD profiles of graphite for the initial two cycles between 0.01 and 1.5 V at $C/40$. (C) GITT profiles of graphite at $C/10$ in the second GPD cycle. (D) dQ/dV profiles corresponding to (B). (E) Rate performance and (F) Cycling performance of graphite at $C/2$.

To reveal the potassium storage mechanism in graphite, we carried out *ex situ* XRD for selected states of charge (SOCs) in the first-cycle GPD at $C/10$ (Figure 2A and B). Upon potassiation, graphite diffraction peaks do not vanish until a certain point between 0.3 and 0.2 V, where new peaks at 22.0° and 29.4° appear, which are attributed to KC_{36} , the stage-three K-GIC (Point 4). In KC_{36} , one layer of potassium appears in every third pair of host graphenes (see Figure 2C).³⁰ Upon further potassiation, KC_{36} transforms to KC_{24} , the stage-two K-GIC, where new peaks at 20.2° and 30.6° are observed (point 5). Finally, after going through a two-phase period (points 6 and 7) to 0.01 V, phase-pure KC_8 , the stage-one K-GIC, forms with characteristic XRD peaks at 16.4° and 33.4° . Similar to KC_8 formed by vapor intercalation, the electrochemically formed KC_8 also shows a golden color (Figure S2). Despite the volume expansion by $\sim 61\%$, a full GPD cycle does convert KC_8 back to graphite via phase

transformations in an opposite direction. The ultimate potassiation product of KC_8 leads a plateau well above the plating potential of potassium metal, which may relieve the danger of dendrite formation. The lowered intensity of broadened XRD peaks of graphite after depotassiation suggests a certain degree of structural damage to graphite caused by the potassium insertion. Interestingly, a shoulder peak near the (002) peak appears upon initial potassiation, disappears at deep potassiation but shows up again after depotassiation beyond the stage-three phase. Further research is being conducted to reveal the phase(s) that corresponds to this shoulder peak. The *ex situ* XRD results, for the first time, show the staging-behavior of K-GICs in a K/graphite cell.

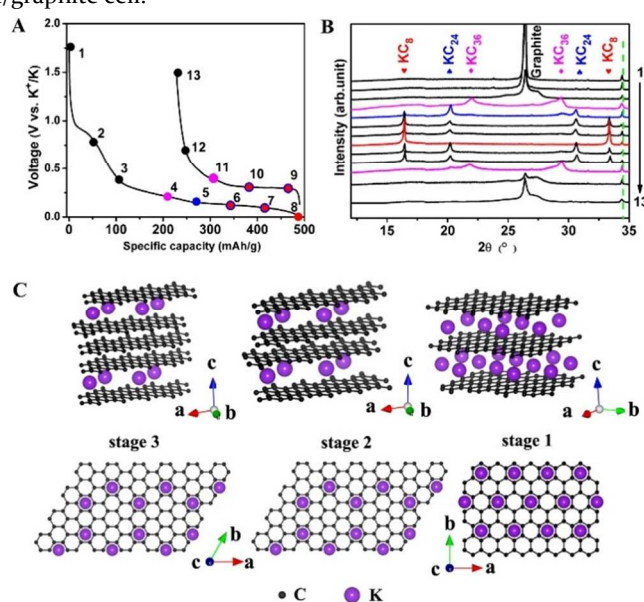


Figure 2. (A) The first-cycle GPD potential profiles at $C/10$. (B) XRD patterns of electrodes corresponding to the marked SOC in (A). (C) Structure diagrams of different K-GICs, side view (up) and top view (down).

Graphite can exhibit a large capacity at low current rates but its capacity drops dramatically upon high rates, as capacities of 263, 234, 172, and 80 mAh/g are obtained at $C/10$, $C/5$, $C/2$, and $1C$, respectively (Figure 1E). Unfortunately, over 50 cycles at $C/2$, the capacity of graphite fades from 197 to 100 mAh/g (Figure 1F). In cycling, we also notice that the CE promptly increases to 93.5% in the second cycle and eventually stabilizes at $\sim 99\%$. This phenomenon of rising CE values indicates the SEI formation during the initial cycling.

Looking at the capacity fading of graphite, we hypothesize that it may be related to the dramatic volume expansion of the compact graphite structure. It is intriguing to test a carbon with a less compact structure, i.e., of a much lower density. Along this line, soft carbon is best situated to test this hypothesis as its less crystalline structure exhibits a much lower density than graphite. We synthesized a soft carbon by pyrolysis of an organic aromatic compound, 3,4,9,10-perylene-tetracarboxylic acid-dianhydride (PTCDA), where the planar aromatic molecules are stacked into a highly crystalline monoclinic structure (Figure S3). The aromaticity of PTCDA certainly helps its graphitizability, as annealing at 1600°C induces a well-defined graphitic order (Figure S4).

We investigate the performance of a representative soft carbon-pyrolyzed PTCDA annealed at 900 °C. This temperature is high enough to remove most of non-carbon elements in PTCDA but low enough not to crystallize the carbon structure. Most importantly, this carbon exhibits a low density of 1.6 g/cc vs. 2.3 g/cc of graphite. Compared to graphite, the (002) XRD peak of soft carbon is much broadened (Figure 3A), which shifts to a lower angle, revealing a larger average d-spacing of 0.355 nm. A representative TEM image reveals the turbostratic structure of this soft carbon (Figure S5). The corresponding selected area electron diffraction (SAED) presents halo rings, indicating its polycrystalline nature with a short-range order (inset of Figure S5). Wide bands and high intensity ratio of D-band over G-band in Raman spectrum corroborate the less graphenic carbon structure (Figure S6).

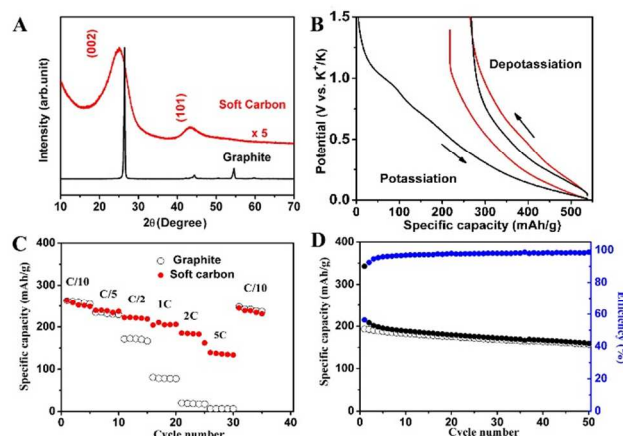


Figure 3. (A) XRD pattern of soft carbon compared with graphite. (B) GPD profiles of soft carbon for the initial two cycles between 0.01 and 1.5 V at C/40. (C) Rate performance of soft carbon; and (D) cycling performance of soft carbon at 2C.

Compared to graphite, soft carbon exhibits very different GPD potential profiles, where only slopes exist instead of plateaus, as shown in Figure 3B, which is also observed in sodiation of soft carbon. The cause for sloping instead of plateau is under investigation. This carbon also exhibits a high depotassiation capacity of 273 mAh/g at C/40, an interesting coincidence since it is the same as graphite. The rate capability of soft carbon is very impressive (Figure 3C). At 1C and 2C, soft carbon exhibits very high capacities of 210 and 185 mAh/g, respectively, compared with 264 mAh/g at C/10. Even at 5C (1395 mA/g), the soft carbon still retains a capacity of 140 mA/g. All GPD potential profiles at different rates show the similar slope behavior (Figure S7). Such high-rate behavior is comparable to the best rate capability of carbon materials in NIBs.^{18, 31} In contrast to the fast capacity fading of graphite anode, soft carbon exhibits much improved cyclability with a capacity retention of 81.4% after 50 cycles at 2C (Figure 3D). Its CE values increases from 56.4% in the first cycle to 92.4% in the second cycle and eventually stabilizes at ~99%. In terms of capacity fading for both K/graphite and K/soft carbon cells, the fading mechanism of carbon electrodes in KIBs is currently unclear; however, it may be related to the decomposition of the electrolyte during the repetitive potassium metal plating and stripping processes. We opened K-graphite cells after 50

cycles and observed that the separator turns yellowish (Figure S8). In future work, electrolyte optimization and pre-potassiation will be carried out to improve the cycling performance and CEs.

In summary, we, for the first time, reveal that potassium can be reversibly inserted into graphite with a high capacity of 273 mAh/g in electrochemical cells. Revealed by *ex situ* XRD, we discovered that upon potassiation, the stage-one KC₈ forms via stage-three KC₃₆ and stage-two KC₂₄ as intermediate phases, where the phase transformations are reversible in converting KC₈ back to a less crystalline graphite. Graphite in KIBs suffers fast capacity fading and moderate rate capability, which may be due to the large volume change over cycling. To further improve the performance, we investigate a low-density soft carbon as a KIB anode, which exhibits much improved cycling life and very high rate capability. The new results fill up important knowledge gaps on carbon electrodes in alkali metal ion batteries and may open up a completely new paradigm for energy storage solutions.

ASSOCIATED CONTENT

Supporting Information

Experimental section, Raman, XRD, TEM, digital photo, molecular structure of PTCDA and potassiation/depotassiation potential profiles at various rates. The Supporting Information is available free of charge on the ACS Publications website at DOI: XXXXXXXX.

AUTHOR INFORMATION

Corresponding Author

*david.ji@oregonstate.edu

Notes

The authors declare no competing financial interests.

ACKNOWLEDGMENT

We acknowledge the financial supports from Oregon State University and Advanced Research Projects Agency-Energy (ARPA-E), Department of Energy of the United States, Award number: DE-AR0000297TDD. We thank Mr. Clement Bomnier, Dr. Wenze Han and Dr. Yang Sun for their discussion. We thank Professor Michael M. Lerner for providing the graphite samples and discussion. The authors are grateful to Professor Douglas A. Keszler for *ex situ* XRD measurements and Professor Chih-Hung Chang for Raman measurements.

REFERENCES

- (1) Nagaura, T.; Tozawa, K. *Prog. Batteries Solar Cells* 1990, 9, 209.
- (2) Dunn, B.; Kamath, H.; Tarascon, J.-M. *Science* 2011, 334, 928.
- (3) Tarascon, J.-M. *Nat. Chem.* 2010, 2, 510.
- (4) Lin, M.-C.; Gong, M.; Lu, B.; Wu, Y.; Wang, D.-Y.; Guan, M.; Angell, M.; Chen, C.; Yang, J.; Hwang, B.-J. *Nature* 2015, 520, 5.
- (5) Liang, Y.; Chen, Z.; Jing, Y.; Rong, Y.; Facchetti, A.; Yao, Y. J. *Am. Chem. Soc.* 2015, 137, 4956.
- (6) <http://pubs.usgs.gov/fs/2002/fso87-02/>.
- (7) Berthelot, R.; Carlier, D.; Delmas, C. *Nature materials* 2011, 10, 74.
- (8) Xia, X.; Dahn, J. *Electrochem. and Solid-State Lett.* 2011, 15, A1.

- (9) Yabuuchi, N.; Kajiyama, M.; Iwatate, J.; Nishikawa, H.; Hitomi, S.; Okuyama, R.; Usui, R.; Yamada, Y.; Komaba, S. *Nat. mater.* 2012, 11, 512.
- (10) Jian, Z.; Zhao, L.; Pan, H.; Hu, Y.-S.; Li, H.; Chen, W.; Chen, L. *Electrochem. Commun.* 2012, 14, 86.
- (11) Wang, L.; Lu, Y.; Liu, J.; Xu, M.; Cheng, J.; Zhang, D.; Goode-nough, J. B. *Angew. Chem. Int. Ed.* 2013, 52, 1964.
- (12) William III, A. *Energy Environ. Sci.* 2015, 8, 540.
- (13) Yabuuchi, N.; Kubota, K.; Dahbi, M.; Komaba, S. *Chem. rev.* 2014, 114, 11636.
- (14) Fong, R.; von Sacken, U.; Dahn, J. *Electrochem. Soc.* 1990, 137, 2009.
- (15) Ohzuku, T.; Iwakoshi, Y.; Sawai, K. J. *Electrochem. Soc.* 1993, 140, 2490.
- (16) Asher, R.; Wilson, S. *Nature* 1958, 181.
- (17) Ge, P.; Fouletier, M. *Solid State Ionics* 1988, 28, 1172.
- (18) Wen, Y.; He, K.; Zhu, Y.; Han, F.; Xu, Y.; Matsuda, I.; Ishii, Y.; Cumings, J.; Wang, C. *Nat. Commun.* 2014, 5.
- (19) Liu, D.; Yang, Z.; Li, W. *Journal of The Electrochemical Society* 2010, 157, D417.
- (20) Liu, D.; Yang, Z.; Li, W.; Qiu, S.; Luo, Y. *Electrochim Acta* 2010, 55, 1013.
- (21) Liu, Y.; Fan, F.; Wang, J.; Liu, Y.; Chen, H.; Jungjohann, K. L.; Xu, Y.; Zhu, Y.; Bigio, D.; Zhu, T.; Wang, C. *Nano letters* 2014, 14, 3445.
- (22) Schleede, A.; Wellmann, M. *Z. Phys. Chem. B* 1932, 18, 1.
- (23) Viculis, L. M.; Mack, J. J.; Mayer, O. M.; Hahn, H. T.; Kaner, R. B. *J. Mater. Chem.* 2005, 15, 974.
- (24) Mizutani, Y.; Abe, T.; Inaba, M.; Ogumi, Z. *Syn. Met* 2001, 125, 153.
- (25) Mizutani, Y.; Abe, T.; Ikeda, K.; Ihara, E.; Asano, M.; Harada, T.; Inaba, M.; Ogumi, Z. *Carbon* 1997, 35, 61.
- (26) Eftekhari, A. J. *Power Sources* 2004, 126, 221.
- (27) Wessells, C. D.; Peddada, S. V.; Huggins, R. A.; Cui, Y. *Nano lett.* 2011, 11, 5421.
- (28) Peled, E. J. *Electrochemical Society* 1979, 126, 2047.
- (29) Winter, M.; Besenhard, J. O.; Spahr, M. E.; Novak, P. *Adv. Ma-ter.* 1998, 10, 725.
- (30) Chacón-Torres, J. C.; Wirtz, L.; Pichler, T. *phys. status solidi B* 2014, 251, 2337.
- (31) Bommier, C.; Ji, X. *Israel J. Chem.* 2015, 55, 486.

SYNOPSIS TOC

